Electronic Supplementary Material (ESI) for Journal of Materials Chemistry A.
This journal is © The Royal Society of Chemistry 2024

Electronic Supplementary Information

Na/TM-Site Mg Substituted P2-$Na_{2/3}[Fe_{1/3}Mg_{1/12}Mn_{7/12}]O_2$ Cathode with Extremely High Capacity for Sodium-Ion Batteries

Ming-Hui Cao,*[a] Ren-Yan Li,[a] Qing-Wen Sun,[a] Miao Cui,[a] Ze-Wei Guo,[a] Lu Ma,[b] Zulipiya Shadike,*[c] and Zheng-Wen Fu*[d]

[a] School of Chemistry and Materials, East China University of Technology, Nanchang, 330013, China

E-mail: mhcao@ecut.edu.cn

[b] National Synchrotron Light Source II, Brookhaven National Laboratory, Upton, NY11973, USA

[c] Institute of Fuel Cells, School of Mechanical Engineering, Shanghai Jiao Tong University, Shanghai, 200240, China

E-mail: zshadike@sjtu.edu.cn

[d] Department of Chemistry, Fudan University, Shanghai, 200433, China

E-mail: zwfu@fudan.edu.cn

Table S1. Stoichiometry from inductively coupled plasma optical emission spectrometry/mass spectrometry (ICP-OES/MS) results of NFMM-1.

Elements	Content(mg/kg)	mol ratio
Na	16.19	0.65(7)
Fe	19.98	0.33(4)
Mg	0.27	0.03(8)
Mn	36.40	0.62(3)

Table S2. Stoichiometry from inductively coupled plasma optical emission spectrometry/mass spectrometry (ICP-OES/MS) results of NFMM-2.

Elements	Content(mg/kg)	mol ratio
Na	16.31	0.66(2)
Fe	19.68	0.32(9)
Mg	0.52	0.08(1)
Mn	29.40	0.58(4)

Table S3. Stoichiometry from inductively coupled plasma optical emission spectrometry/mass spectrometry (ICP-OES/MS) results of NFMM-3.

Elements	Content(mg/kg)	mol ratio
Na	16.24	0.65(8)
Fe	19.44	0.32(5)
Mg	1.02	0.16(4)
Mn	34.06	0.49(8)

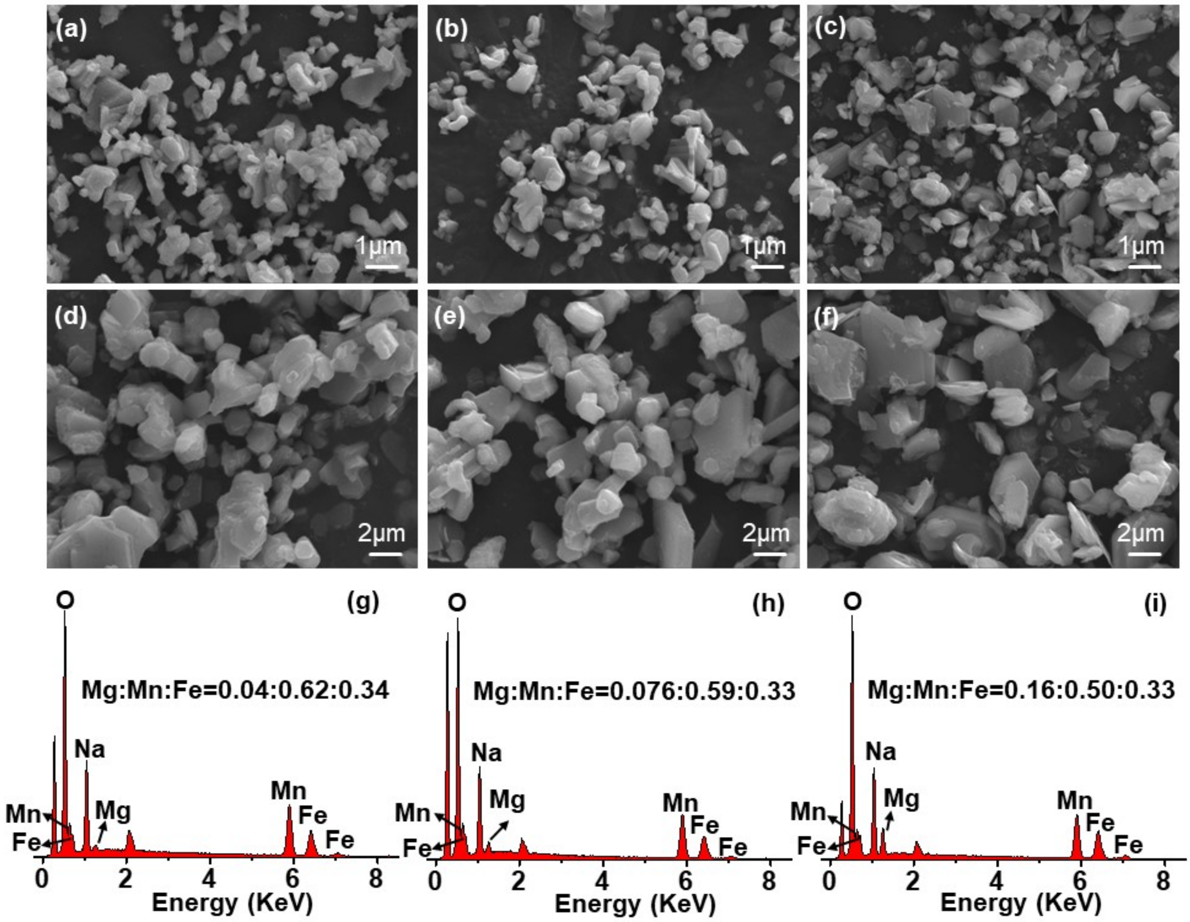

Fig. S1. Low magnification SEM images of (a) NFMM-1, (b) NFMM-2 and (c) NFMM-3 powders. High magnification SEM images of (d) NFMM-1, (e) NFMM-2 and (f) NFMM-3 powders. EDX analysis of (g) NFMM-1, (h) NFMM-2 and (i) NFMM-3 powders. Note that the ratios in EDX are atomic ratios.

Table S4. Refined crystallographic parameters by Rietveld analysis for NFMM-1. S.G. *P63/mmc*, $a = b =$ 2.90(9) Å, $c = 11.26(8)$ Å, $\alpha = \beta = 90°$, $\gamma = 120°$, R_{wp}=3.07%, $\chi^2 = 0.3565$.

Atom	Site	*x*	*y*	*z*	Occupancy	Uiso
Na1	*2b*	0	0	0.25	0.3776	1.4(5)
Na2	*2d*	0.3333	0.6667	0.75	0.3045	1.4(7)
Mg	*2a*	0	0	0	0.0385	0.76(3)
Fe	*2a*	0	0	0	0.3333	0.51(2)
Mn	*2a*	0	0	0	0.6222	0.39(1)
O	*4f*	0.3333	0.6667	0.0872	0.9835	0.74(2)
P63/mmc : $a = b = 2.9095(3)$ Å c =11.2681(7) Å V= 82.71(6) Å^3						
D（Na）=3.6688 Å D（TM）=1.9652 Å						
$R_p = 2.41\%$ R_{wp} =3.07% GOF(χ^2) = 0.3565						

Rietveld refinement was conducted using hexagonal space group P63/mm and by placing ~ 3.85 mol % Mg ions in transition-metal layer. The refinement shows excellent goodness of fit with this model (GOF(χ^2) = 0.3565), which confirms the proposed structural model.

Table S5. Refined crystallographic parameters by Rietveld analysis for NFMM-2. S.G. *P63/mmc*, $a = b =$ 2.91(8) Å, c = 11.27(7) Å, $\alpha = \beta = 90°$, $\gamma = 120°$, R_{wp}=2.29%, $\chi^2 = 0.3221$.

Atom	Site	*x*	*y*	*z*	Occupancy	Uiso
Na1	*2b*	0	0	0.25	0.2623	1.7(5)
Na2	*2d*	0.3333	0.6667	0.75	0.4622	1.7(8)
Mg1	*2a*	0	0	0	0.0689	0.68(1)
Mg2	*2d*	0.3333	0.6667	0.75	0.0123	0.35(2)
Fe	*2a*	0	0	0	0.3333	0.24(2)
Mn	*2a*	0	0	0	0.6171	0.25(8)
O	*4f*	0.3333	0.6667	0.0872	0.9973	0.79(3)
P63/mmc : $a = b$ = 2.9184(5) Å c =11.2779(3) Å V= 83.18(3) Å^3						
D（Na）=3.7690 Å D（TM）=1.9849 Å						
R_p = 1.82% R_{wp} =2.29% GOF(χ^2) = 0.3221						

Rietveld refinement was conducted using hexagonal space group P63/mm and by placing Mg ions in transition-metal layer (~6.89 mol %) and Na layer (~1.23 mol %). The refinement shows excellent goodness of fit with this model (GOF(χ^2) = 0.3221), which confirms the proposed structural model.

Table S6. Refined crystallographic parameters by Rietveld analysis for NFMM-3. S.G. *P63/mmc*, $a = b =$ 2.92(3) Å, c = 11.25(5) Å, $\alpha = \beta = 90°$, $\gamma = 120°$, R_{wp}=9.05%, $\chi^2 = 0.8274$.

Atom	Site	*x*	*y*	*z*	Occupancy	Uiso
Na1	*2b*	0	0	0.25	0.2503	2.3(3)
Na2	*2d*	0.3333	0.6667	0.75	0.4025	2.3(3)
Mg1	*2a*	0	0	0	0.1270	0.88(4)
Mg2	*2d*	0.3333	0.6667	0.75	0.0368	0.46(2)
Fe	*2a*	0	0	0	0.3333	0.34(7)
Mn	*2a*	0	0	0	0.4972	0.35(6)
O	*4f*	0.3333	0.6667	0.0872	0.9969	0.89(8)
P63/mmc : $a = b$ = 2.9231(8) Å c =11.2558(4) Å V= 83.28(2) Å^3						
D (Na)=3.5682 Å D (TM)=2.0647 Å						
R_p = 6.98% R_{wp} =9.05% GOF(χ^2) = 0.8274						

Rietveld refinement was conducted using hexagonal space group P63/mm and by placing Mg ions in transition-metal layer (~12.70 mol %) and Na layer (~3.68 mol %). The refinement shows excellent goodness of fit with this model (GOF(χ^2) = 0.8274), which confirms the proposed structural model.

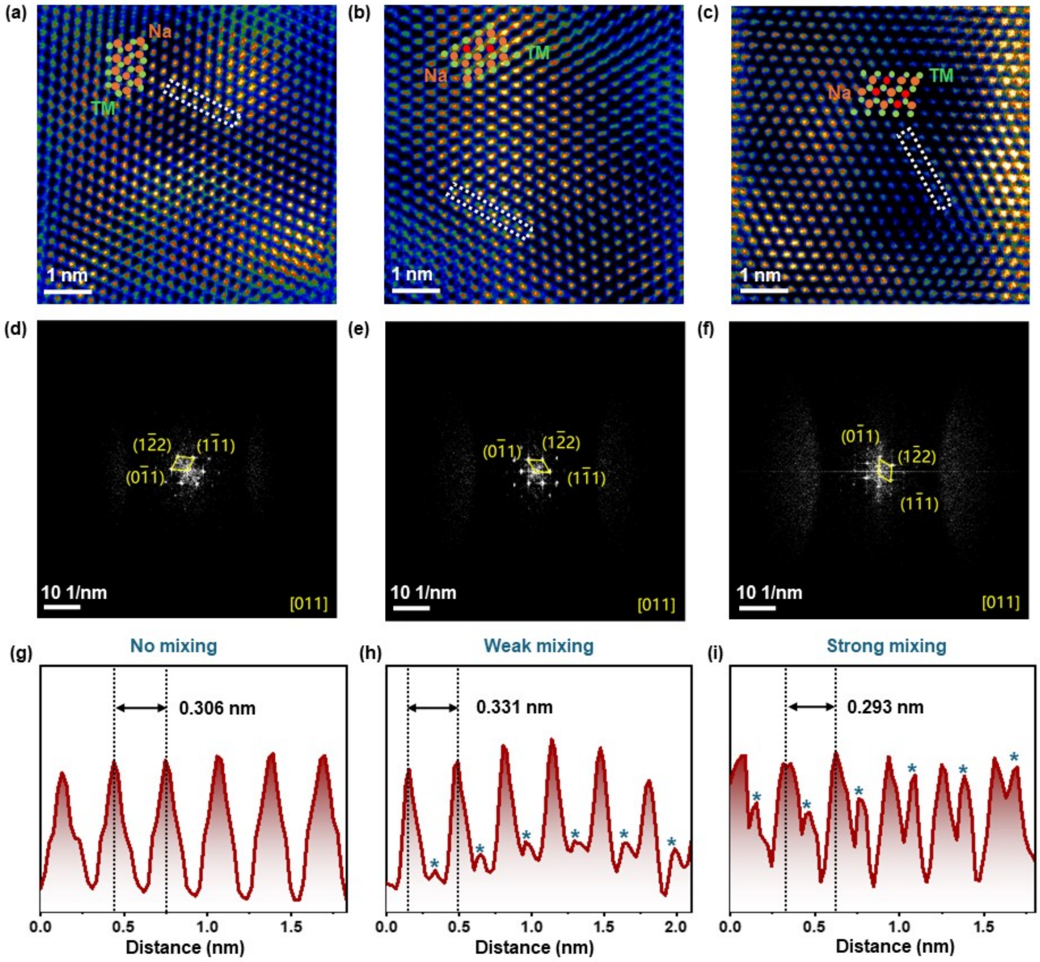

Fig. S2. HAADF-STEM images of the pristine (a) NFMM-1, (b) NFMM-2 and (c) NFMM-3 particles viewed along the [011] direction. (d-e) The corresponding FFT patterns for a-c. (g-i) The line scan profiles along the corresponding rectangles in a-c (note that the insets in a-c are the schematic structural diagrams, legend: orange (Na), red (Na_{Mg}) and green (Mg/Fe/Mn)).

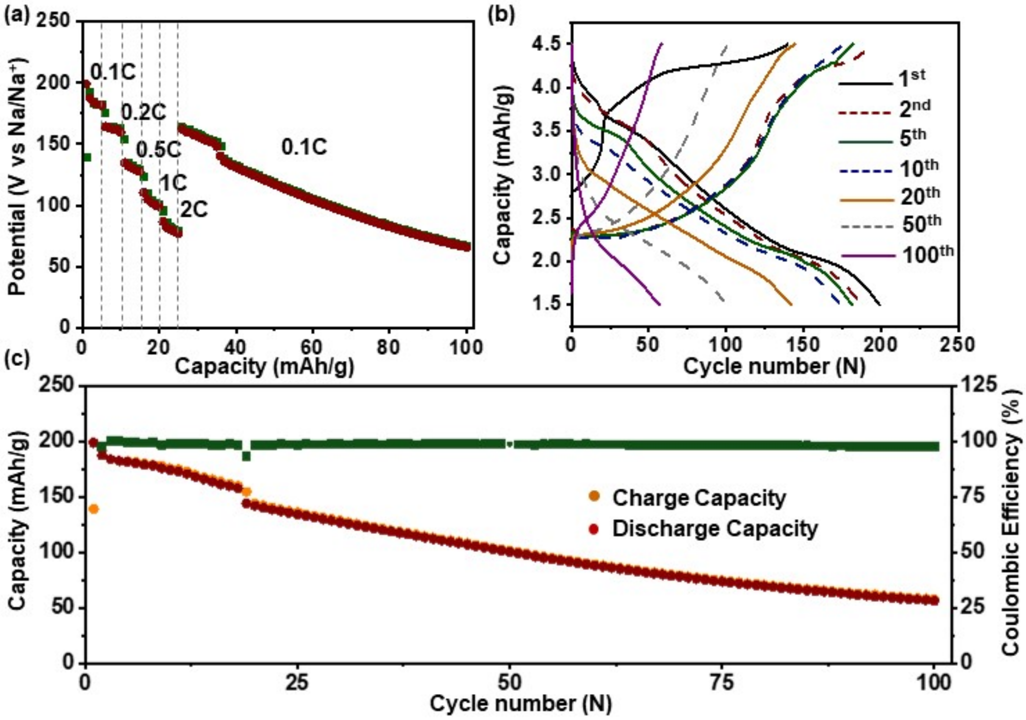

Fig. S3. Electrochemical performance of $Na_{2/3}Fe_{1/3}Mn_{2/3}O_2$ cathode with mass loading of ~2 mg cm^{-2} in the voltage range of 1.5-4.5 V vs. Na^+/Na. (a) Rate capability (0.1C-2C) in the voltage range of 1.5-4.5 V, (b) Representative charge/discharge curves of NFMM cathode at 0.1C in the voltage range of 1.5-4.5 V, (c) Charge/discharge capacity and Coulombic efficiency as a function of cycle number.

To facilitate comparison, the $Na_{2/3}Fe_{1/3}Mn_{2/3}O_2$ cathode (denoted as NFMM) was synthesized and its electrochemical performance was evaluated in a Na-half cell. The cathode mass loading is ~2 mg cm^{-2}. From Fig. S3, it can be observed that compared to the NFMM-2 cathode, the NFMM cathode exhibits inferior rate capability and cycling stability. Specifically, under a high current rate of 2C, the reversible capacities of the NFMM cathode are only 76.99 mAh g^{-1}, which is approximately 38.69% of the initial reversible capacity (198.99 mAh g^{-1}). Additionally, after reducing the current rate back to 0.1C, there is a rapid decay in capacity for this material with a capacity retention of only 33.05% after 100 cycles. As for cycle stability, after 100 cycles, the NFMM cathode retains a low capacity of merely 56.74 mAh g^{-1} and demonstrates a capacity decay rate of approximately 0.71% per cycle.

Table S7. Comparison of the electrochemical properties of Mg-doped layered cathode materials for sodium ion batteries based on anionic redox.

Electrode materials	Voltage range (V)	Initial reversible capacity (mAh/g)	Coulombic Efficiency of the 2nd cycle	Capacity at high-rate (mAh/g)	Capacity retention After cycling	Reference
P2-$Na_{0.6}Mg_{0.3}Mn_{0.7}O_2$	1.5-4.4	210 (0.05C)	97.9%	52 (2C)	50% (0.05C, 50 cycles)	S1
P2-$Na_{2/3}Mg_{0.28}Mn_{0.72}O_2$	2.0-4.5	150 (0.1C)	100%	/	/	S2
P2-$Na_{2/3}Mg_{1/3}Mn_{2/3}O_2$	2.0-4.5	164 (0.1C)	98.6% (0.2C)	125 (1C)	80% (1C, 100 cycles)	S3
P3-$Na_{2/3}Mg_{1/3}Mn_{2/3}O_2$.	1.6-4.4	222 (0.05C)	95.45% (0.05C)	75 (2C)	76.5% (0.1C, 30 cycles)	S4
P2-$Na_{0.67}Mg_{0.2}Mn_{0.8}O_2$	1.8-3.8	158 (0.1C)	96.7%	107 (5C)	96% (0.1C, 25 cycles)	S5
P2-$Na_{2/3}[Mn_{7/9}Mg_{1/9}\square_{1/9}]O_2$	1.5-4.5	212 (0.1C)	83% (2.1-4.4 V)	87(1C 2.1-4.4 V)	No capacity fading (0.1C, 50 cycles)	S6
P2-$Na_{0.63}[\square_{0.036}Mg_{0.143}Mn_{0.820}]O_2$	1.5-4.5	198 (0.05C)	97%	/	/	S7
P2-$Na_{0.7}Mn_{0.6}Ni_{0.2}Mg_{0.2}O_2$	1.5-4.2	130 (0.2C)	96.6%	72 (2C, 2.5-4.2 V)	79% (1C, 1000 cycles)	S8
P2-$Na_{0.773}Mg_{0.03}Li_{0.25}Mn_{0.75}O_2$	2.0-4.5	192 (15 mA/g)	97%	119 (600 mA/g)	59.7% (20 mA/g, 100 cycles, 2.6-4.5 V)	S9
P2-$Na_{0.67}Mg_{0.1}Zn_{0.1}Mn_{0.8}O_2$	1.5-4.5	230 (0.1C)	/	125 (5C)	71.7% (0.1C, 50 cycles)	S10
P2-$Na_{0.6}Mg_{0.15}Mn_{0.7}Cu_{0.15}O_2$	2.0-4.5	157 (0.1C)	/	88.5 (2C)	95.8% (1C, 200 cycles)	S11
P2-$Na_{2/3}Mn_{0.72}Cu_{0.22}Mg_{0.06}O_2$	2.0-4.5	107.6 (0.1C)	97%	87.4 (2C)	87.9% (1C, 100 cycles)	S12
P2-$Na_{0.75}Li_{0.2}Mg_{0.05}Al_{0.05}Mn_{0.7}O_2$	1.5-4.5	245 (0.05C)	93.8%	80 (2C)	54% (0.05C, 50 cycles)	S13
P2-$Na_{0.84}Mn_{0.67}Ni_{0.3-x}Mg_x\square_{0.03}O_2$	1.8-4.4	153 (0.1C)	/	117.3 (2C)	98.3% (0.1C, 50 cycles)	S14
P2-$Na_{0.66}Li_{0.18}Mn_{0.71}Mg_{0.21}Co_{0.08}O_2$	1.5-4.5	166 (0.1C)	97%	110.8 (1C)	82% (0.1C, 100 cycles)	S15
P2-$Na_{0.67}Mn_{0.71}Cu_{0.02}Mg_{0.02}Ni_{0.25}O_2$	1.5-4.5	152 (0.1C)	/	108 (2C)	86% (0.1C, 100 cycles)	S16
P2-$Na_{2/3}[Fe_{1/3}Mg_{1/12}Mn_{7/12}]O_2$	**1.5-4.5**	**253 (0.1C)**	**98.54%**	**115.44 (2C)**	**50.8% (0.1C, 100 cycles)**	**This work**

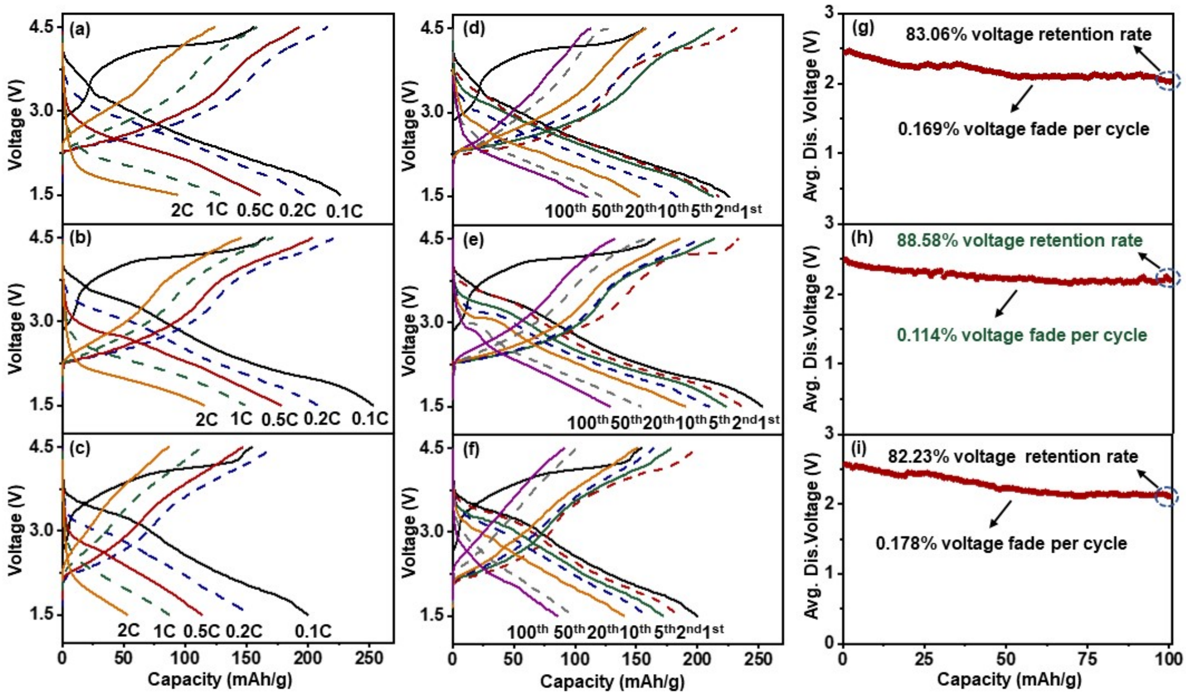

Fig. S4. Electrochemical performance of $Na_{2/3}[Fe_{1/3}Mg_xMn_{2/3-x}]O_2$ cathode with mass loading of ~2 mg/cm^{-2} in the voltage range of 1.5-4.5 V vs. Na^+/Na. The charge/discharge profiles at different current rates (0.1C-2C) of the (a) NFMM-1, (b) NFMM-2 and (c) NFMM-3 electrodes in the voltage range of 1.5-4.5 V vs. Na^+/Na. Typical galvanostatic charge/discharge profiles (1st, 2nd, 5th, 10th, 20th,50th, 100th) of the (d) NFMM-1, (e) NFMM-2 and (f) NFMM-3 electrodes at 0.1C in the voltage range of 1.5-4.5 V. Average discharge voltage vs. cycle number plots of the (g) NFMM-1, (h) NFMM-2 and (i) NFMM-3 electrodes within 100 cycles.

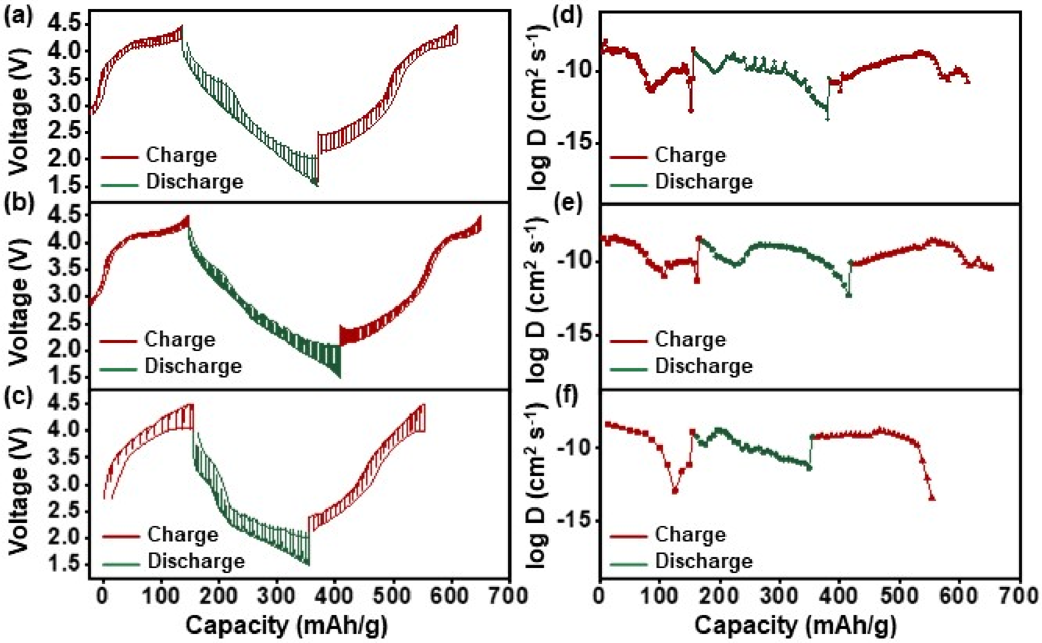

Fig. S5. The transient voltage response of (a) NFMM-1, (b) NFMM-2 and (c) NFMM-3 electrodes during GITT for the first cycle and second charge between 1.5 and 4.5 V versus Na^+/Na; Calculated D_{Na+} of (d) NFMM-1, (e) NFMM-2 and (f) NFMM-3 electrodes.

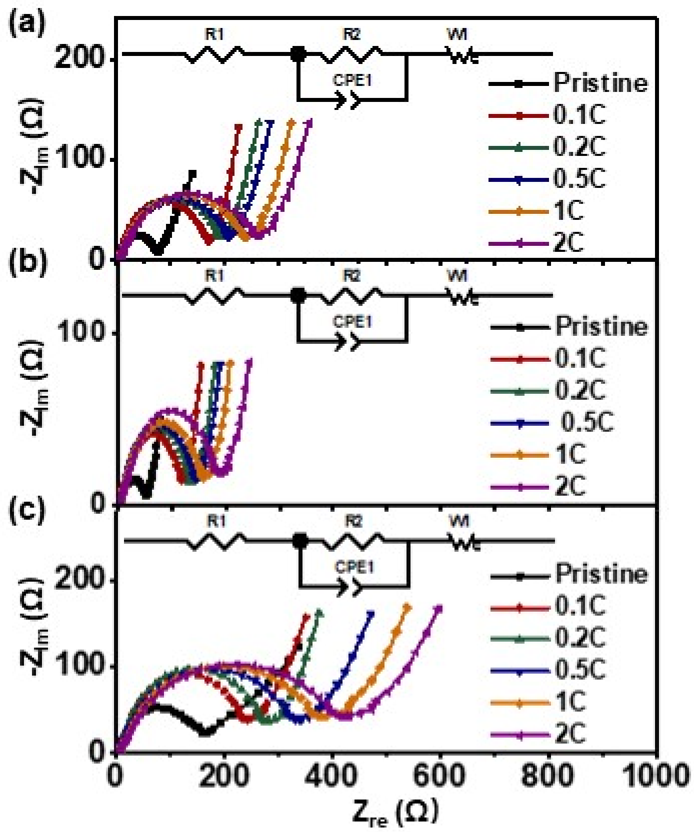

Fig. S6. (a) EIS results of the (a) NFMM-1, (b) NFMM-2 and (c) NFMM-3 electrodes during rate performance testing.

Table S8. Fitting results of the impedance parameters and the corresponding ion conductivities of the (a) NFMM-1, (b) NFMM-2, and (c) NFMM-3 electrodes during rate performance testing.

Samples	**State**	**R_e (Ω)**	**R_{ct} (Ω)**	**σ (S cm^{-1})**
NFMM-1	Pristine	4.09	84.95	1.22×10^{-5}
	0.1C	4.46	195.62	5.31×10^{-6}
	0.2C	4.77	221.48	4.69×10^{-6}
	0.5C	5.51	240.49	4.32×10^{-6}
	1C	5.98	268.81	3.86×10^{-6}
	2C	6.04	288.64	3.60×10^{-6}
NFMM-2	Pristine	4.02	57.59	1.80×10^{-5}
	0.1C	4.48	132.28	7.85×10^{-6}
	0.2C	4.70	149.12	6.97×10^{-6}
	0.5C	5.07	160.47	6.47×10^{-6}
	1C	5.14	174.28	5.96×10^{-6}
	2C	5.53	203.97	5.09×10^{-6}
NFMM-3	Pristine	4.15	184.59	5.63×10^{-6}
	0.1C	4.74	295.31	3.52×10^{-6}
	0.2C	5.41	349.29	2.97×10^{-6}
	0.5C	5.84	371.54	2.80×10^{-6}
	1C	6.05	406.20	2.56×10^{-6}
	2C	6.39	440.67	2.36×10^{-6}

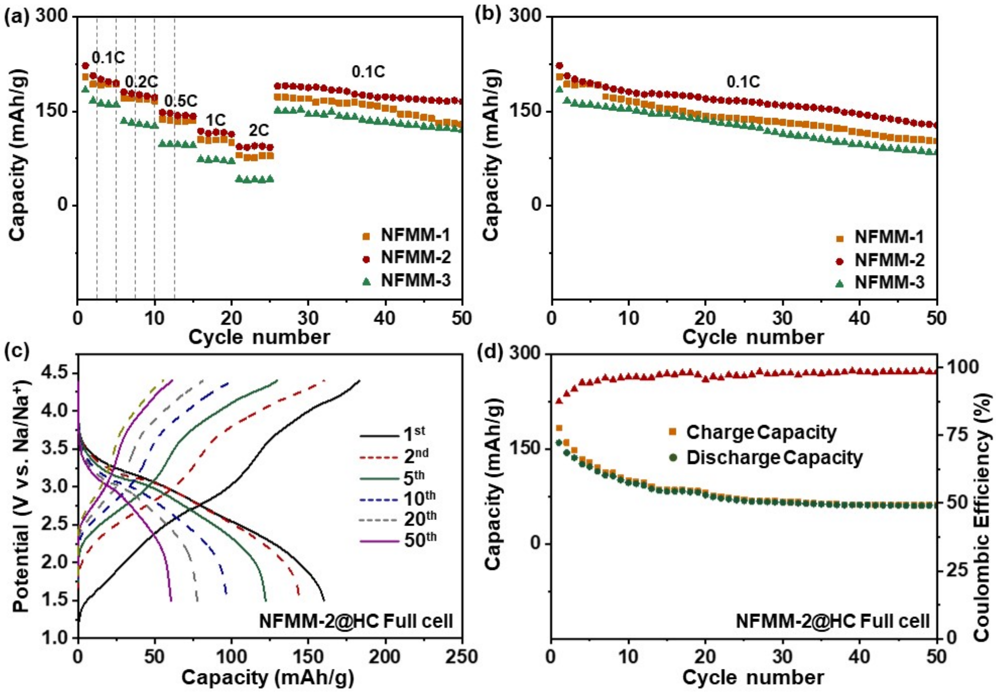

Fig. S7. Electrochemical performance of $Na_{2/3}[Fe_{1/3}Mg_xMn_{2/3-x}]O_2$ cathode with mass loading of ~5 mg cm^{-2}. (a) Rate capability (0.1-2C) of the NFMM-1, NFMM-2 and NFMM-3 electrodes in the potential range of 1.5-4.5 V versus Na^+/Na. (b) Cycle performance of the NFMM-1, NFMM-2 and NFMM-3 electrodes in the potential range of 1.5-4.5 V versus Na^+/Na. (c) Typical charge/discharge curves of the NFMM-2@HC full cell cycled between 1.5 and 4.4 V at a 0.1C rate. (d) The charge/discharge capacity and coulombic efficiency versus cycle number at the 0.1C rate for the NFMM-2@HC full cell. Note that the specific capacities were calculated based on the mass of cathode material.

Compared to batteries with lower cathode mass loading (~2 mg/cm^2), the overall electrochemical performance of NFMM-1, NFMM-2, and NFMM-3 electrodes with higher cathode mass loading of ~5 mg/cm^2 is diminished (Figure S7). Specifically, NFMM-1, NFMM-2, and NFMM-3 electrodes exhibit reduced initial charge-discharge capacities of 140.79/204.57, 147.20/222.31, and 136.39/183.43 mAh g^{-1} respectively at 0.1C (Figure S8d-f). Under a high current rate of 2C, the reversible capacities of NFMM-1, NFMM-2, and NFMM-3 electrodes are significantly decreased to 79.53, 92.67 and 42.35 mAh g^{-1} respectively, indicating a decline in high-rate performance (Figure S7a and S8a-c). Furthermore, within 50 cycles, the capacity decay rates for each cycle of the NFMM-1, NFMM-2, and NFMM-3 electrodes reach 0.99%, 0.85%, and 1.10% respectively, suggesting a decrease in cycling performance as well (Figure S7b). From Figure S8g-i, it can be observed that the voltage retention rates of NFMM-1, NFMM-2, and NFMM-3 electrodes after 50 cycles are 85.65%, 87.71%, and 84.52% respectively, indicating a more pronounced voltage decay issue. Additionally, the cycling performance of the full cell with the NFMM-2 electrode decreases to only 35.20% after 50 cycles (Figure S7c-d). These degradation phenomena in performance primarily stem from sluggish electrode kinetics. However, it is important to note that compared to NFMM-1 and NFMM-3, the NFMM-2 still exhibits superior overall electrochemical performance without any fundamental changes in its electrochemical characteristics.

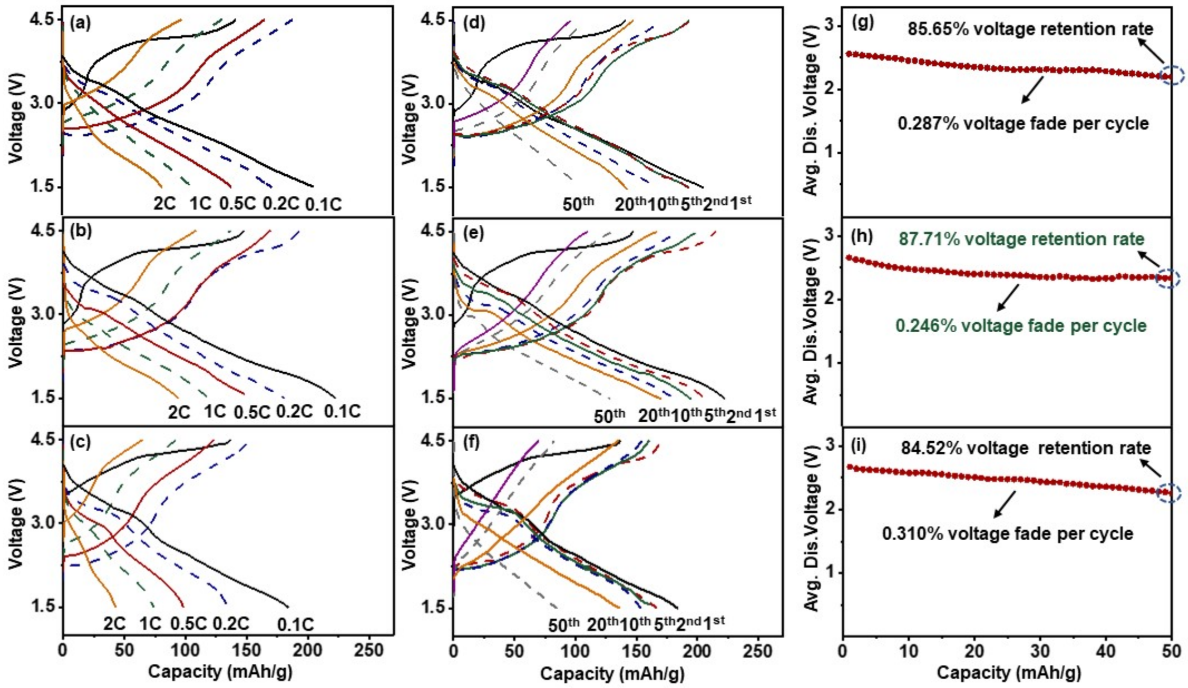

Fig. S8. Electrochemical performance of $Na_{2/3}[Fe_{1/3}Mg_xMn_{2/3-x}]O_2$ cathode with mass loading of ~5 mg cm^{-2}. The charge/discharge profiles at different current rates (0.1C-2C) of the (a) NFMM-1, (b) NFMM-2 and (c) NFMM-3 electrodes in the voltage range of 1.5-4.5 V vs. Na^+/Na. Typical galvanostatic charge/discharge profiles (1st, 2nd, 5th, 10th, 20th, 50th) of the (d) NFMM-1, (e) NFMM-2 and (f) NFMM-3 electrodes at 0.1C in the voltage range of 1.5-4.5 V. Average discharge voltage vs. cycle number plots of the (g) NFMM-1, (h) NFMM-2 and (i) NFMM-3 electrodes within 50 cycles.

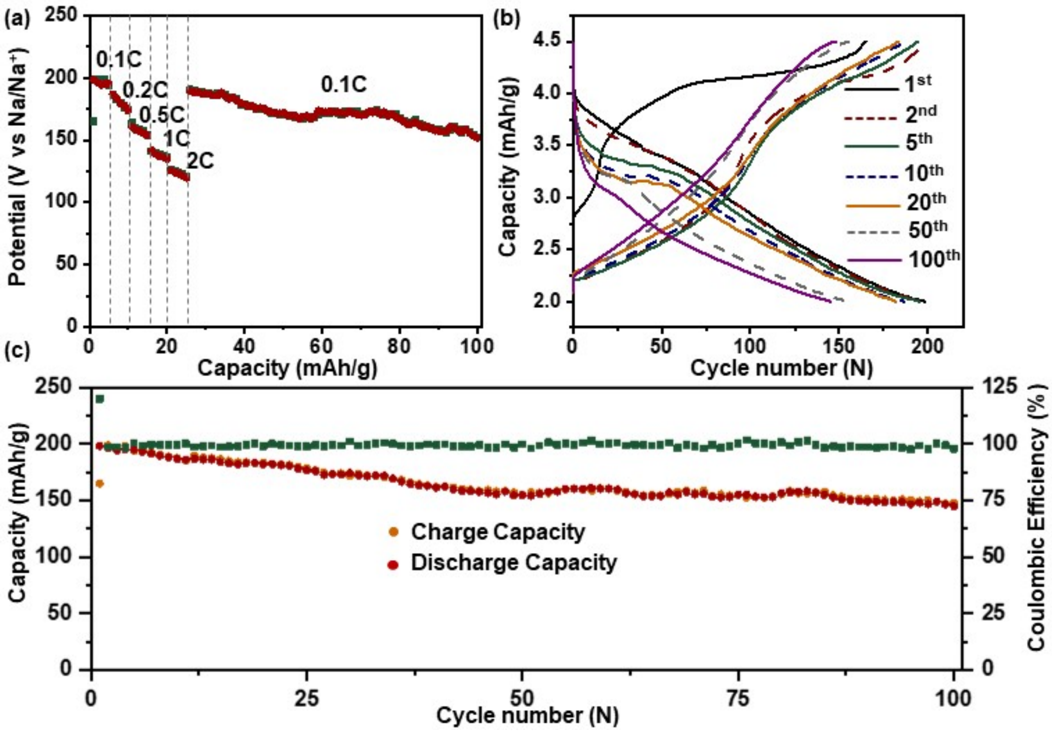

Fig. S9. Electrochemical performance of NFMM-2 cathode with mass loading of ~2 mg cm^{-2} in the voltage range of 2.0-4.5 V vs. Na^+/Na . (a) Rate capability (0.1C-2C) in the voltage range of 2.0-4.5 V, (b) Representative charge/discharge curves of NFMM-2 cathode at 0.1C in the voltage range of 2.0-4.5 V, (c) Charge/discharge capacity and Coulombic efficiency as a function of cycle number.

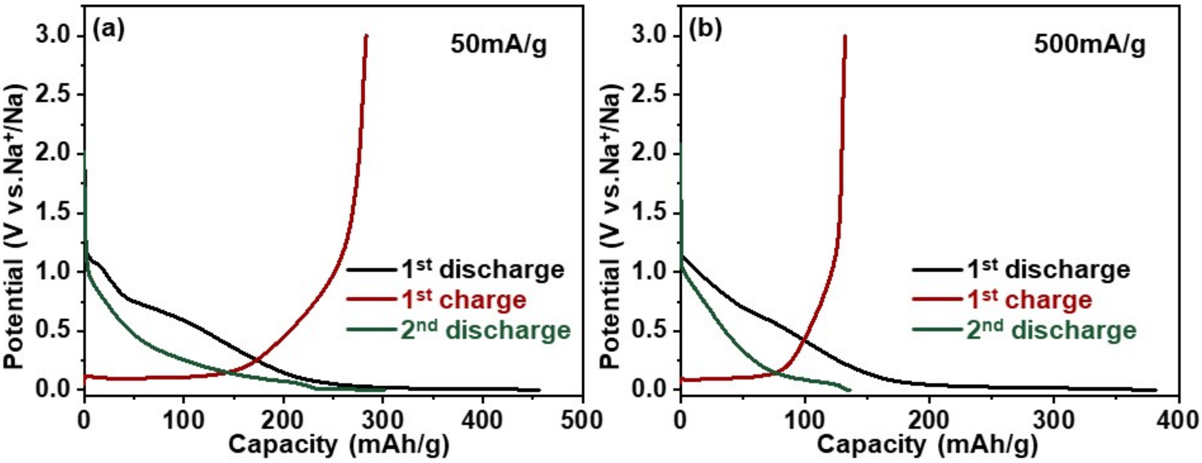

Fig. S10. The initial two charge-discharge curves of hard carbon at current densities of (a) 50 mA g^{-1} and (b) 500 mA g^{-1}, respectively.

References

S1 X. Rong, F. Gao, Y. Lu, K. Yang and Y. Hu, *Chinese Chem. Lett*., 2018, **29**, 1791-1794.

S2 U. Maitra, R. A. House, J. W. Somerville, N. Tapia -Ruiz, J. G. Lozano, N. Guerrini, R. Hao, K. Luo, L. Jin, M. A. Pérez -Osorio, F. Massel, D. M. Pickup, S. Ramos, X. Lu, D. E. McNally, A. V. Chadwick, F. Giustino, T. Schmitt, L. C. Duda, M. R. Roberts and P. G. Bruce, *Nat. Chem*., 2018, **10**, 288-295.

S3 K. Dai, J. Wu, Z. Zhuo, Q. Li, S. Sallis, J. Mao, G. Ai, C. Sun, Z. Li, W. E. Gent, W. C. Chueh, Y. Chuang, R. Zeng, Z. Shen, F. Pan, S. Yan, L. F. J. Piper, Z. Hussain, G. Liu and W. Yang, *Joule*., 2019, **3**, 518-541.

S4 B. Song, E. Hu, J. Liu, Y. Zhang, X. -Q. Yang, J. Nanda V K. Page, *J. Mater. Chem. A*, 2019, **7**, 1491-1498.

S5 E. J. Kim, L. A. Ma, D. M. Pickup, A. V. Chadwick, R. Younesi, P. Maughan, J. T. S. Irvine and A. R. Armstrong, *ACS Appl. Energy Mater*., 2020, **3**, 10423-10434.

S6 L. Yang, Z. Liu, S. Liu, M. Han, Q. Zhang, L. Gu, Q. Li, Z. Hu, X. Wang, H. -J. Lin, C. -T. Chen, J. -M. Chen, S.-C. Haw, Z. Wang and L. Chen, *Nano Energy*., 2020, **78**, 105172.

S7 X. Bai, A. Iadecola, J. -M. Tarascon and P. Rozier, *Energy Storage Mater*., 2020, **31**, 146-155.

S8 Q. -C. Wang, J. -K. Meng, X. -Y. Yue, Q. -Q. Qiu, Y. Song, X. -J. Wu, Z. -W. Fu, Y. -Y. Xia, Z. Shadike, J. Wu, X. -Q. Yang and Y. -N. Zhou, *J. Am. Chem. Soc*., 2019, **141**, 840-848.

S9 Y. Huang, Y. Zhu, A. Nie, H. Fu, Z. Hu, X. Sun, S. -C. Haw, J. -M. Chen, T. -S. Chan, S. Yu, G. Sun, G. Jiang, J. Han, W. Luo and Y. Huang, *Adv. Mater*., 2022, **34**, 2105404.

S10 H. Ji, W. Ji, H. Xue, G. Chen, R. Qi, Z. Huang, H. Fang, M. Chu, L. Liu, Z. Ma, S. Xu, J. Zhai, W. Zeng, C. Schulz, D. Wong, H. Chen, J. Xu, W. Yin, F. Pan and Y. Xiao, *Sci. Bull*., 2023, **68**, 65-76.

S11 C. Cheng, C. Chen, S. Chu, H. Hu, T. Yan, X. Xia, X. Feng, J. Guo, D. Sun, J. Wu, S. Guo and L. Zhang, *Adv. Mater*., 2022, **34**, 2201152.

S12 P. -F. Wang, Y. Xiao, N. Piao, Q. -C. Wang, X. Ji, T. Jin, Y. -J. Guo, S. Liu, T. Deng, C. Cui, L. Chen, Y. -G. Guo, X. -Q. Yang and C. Wang, *Nano Energy*., 2020, **69**, 104474.

S13 X. Chen, C. Cheng, M. Ding, Y. Xia, L. -Y. Chang, T. -S. Chan, H. Tang, N. Zhang and L. Zhang, *ACS Appl. Mater. Interfaces*., 2020, **12**, 43665-43673.

S14 Y. Hou, J. Jin, C. Huo, Y. Liu, S. Deng and J. Chen, *Energy Storage Mater*., 2023, **56**, 87-95.

S15 J. Xiao, F. Zhang, K. Tang, X. Li, D. Wang, Y. Wang, H. Liu, M. Wu and G. Wang, *ACS Cent. Sci*., 2019, **5**, 1937-1945.

S16 W. Kong, R. Gao, Q. Li, W. Yang, J. Yang, L. Sun and X. Liu, *J. Mater. Chem. A*, 2019, **7**, 9099-9109.